Original article

JOURNAL OF REINFORCED PLASTICS & COMPOSITES

Journal of Reinforced Plastics and Composites
2022, Vol. 41(3-4) 130–146

DOI: 10.1177/07316844211050168
journals.sagepub.com/home/jrp
SAGE

Estimating the compressive strength of rectangular fiber reinforced polymer–confined columns using multilayer perceptron, radial basis function, and support vector regression methods

Yaser Moodi[1], Mohammad Ghasemi[2] and Seyed Roohollah Mousavi[1]

Abstract

Recently, there has been a tendency to use machine learning (ML)–based methods, such as artificial neural networks (ANNs), for more accurate estimates. This paper investigates the effectiveness of three different machine learning methods including radial basis function neural network (RBNN), multi-layer perceptron (MLP), and support vector regression (SVR), for predicting the ultimate strength of square and rectangular columns confined by various FRP sheets. So far, in the previous study, several experiments have been conducted on concrete columns confined by fiber reinforced polymer (FRP) sheets with the results suggesting that the use of FRP sheets enhances the compressive strength of concrete columns effectively. Also, a wide range of experimental data (including 463 specimens) has been collected in this study for square and rectangular columns, confined by various FRP sheets. The comparison of ML-derived results with the experimental findings, which were in a very good agreement, demonstrated the ability of ML to estimate the compressive strength of concrete confined by FRP; the correlation coefficient (R^2) for MLP, RBFNN, and SVR methods was equal to 0.97, 0.97, and 0.90, respectively. Similar accuracy was obtained by MLP and RBFNN, and they provided better estimates for determining the compressive strength of concrete confined by FRP. Also, the results showed that the difference between statistical indicators for training and testing specimens in the RBFNN method was greater than the MLP method, and this difference indicated the poor performance of RBFNN.

Keywords

Multilayer perceptron, support vector regression, radial basis function neural network, FRP confinement, compressive strength, strengthening

Introduction

Most of the existing reinforced concrete columns require retrofitting and strengthening for various reasons, including errors during the construction phase, design mistakes, changing the type of applications in structures, corrosion of steel and reinforcement, changes in design codes, the occurrence of strong beam–weak column mechanism, and the damages due to natural disasters such as earthquake, wind, and flood. In addition, the destruction and rebuilding of these columns are costly and often impractical. Note that strengthening and retrofitting techniques are affordable and reliable.[1] FRP is usually used for strengthening the existing reinforced concrete columns. One of the first experimental studies on FRP-confined concrete columns was presented by Nanni and Bradford in 1994.[2] Their specimens included the concrete with ordinary strength, wrapped by three kinds of FRP under uniaxial compressive loading. By investigating stress–strain curves, they indicated that compressive strength and ductility are raised using FRP confinement. Different studies were conducted for estimating the compressive strength of columns wrapped by FRP.[3–15] Note that most of the proposed models were presented by limited specimens in the past.

[1]Civil Engineering Department, University of Sistan and Baluchestan, Zahedan, Iran
[2]Department of Civil Engineering, University of Velayat, Iranshahr, Iran

Corresponding author:
Mohammad Ghasemi, Assistant Professor, Department of Civil Engineering, University of Velayat, Iranshahr, Iran.
Email: m.ghasemi@velayat.ac.ir

Table 1. Methods used to estimate compressive strength of FRP-confined columns.

	Study	Year	Section(s)	Method(s)	Types of concrete	Number of specimens
1	Cevik and Cabalar[31]	2008	Circular	GP	Plain	180
2	Cevik and Guzelbey[32]	2008	Circular	ANN	Plain	101
3	Wu et al.[27]	2010	Rectangular, circular	RBFNN	Plain	154, 362
4	Gandomi et al.[33]	2010	Circular	LGP	Plain	101
5	Naderpour et al.[34]	2010	Circular	ANN-BP	Plain	213
6	Cevik et al.[35]	2010	Circular	GP, SR	Plain	101
7	Cevik[36]	2011	Circular	GP, SR, NF, ANN	Plain	180
8	Elsanadedy et al.[37]	2012	Circular	ANN	Plain	272
9	Jalal and Ramezanianpour[38]	2012	Circular	ANN	Plain	128
10	Jalal et al.[39]	2013	Circular	GP, ANFIS	Plain	128
11	Pham and Hadi[28]	2014	Rectangular	ANN	Plain	209
12	Doran et al.[29]	2015	Rectangular	MFIS	Plain	140
13	Lim et al.[40]	2016	Circular	GP	Plain	832
14	Mansouri et al.[41]	2016	Circular	ANN, ANFIS, MARS, M5Tree	Plain	1153
15	Mozumder et al.[42]	2016	Circular	SVR	Plain	238
16	Cascardi et al.[43]	2017	Circular	ANN	Plain	465
17	Mansouri et al.[44]	2017	Circular	RBNN, ANFIS-SC, ANFIS-FCM, M5Tree	Plain	519
18	Moodi et al.[12]	2018	Rectangular	RSM	Plain	416
19	Sharifi et al.[45]	2019	Rectangular	ANN	Plain	190
20	Naderpour et al.[46]	2019	Circular	ANN, GMDH, GEP	RC	135
21	Mohana[30]	2019	Rectangular	ANN, SVR	RC	163
22	Kamgar et al.[47]	2020	Circular	FFBPNN	Plain	281
23	Hamid et al.[48]	2020	Circular	ANN	RC	49
24	Ahmad et al.[49]	2020	Circular	ANN	Plain	708
25	Keshtegar et al.[50]	2021	Circular	RSM-SVR	Plain	780

Artificial intelligence and soft computing methods, more commonly known as machine learning methods, are widely used nowadays in many fields, especially in civil engineering, as effective methods to link complex experimental data.[16–23] Thus, they are suitable alternatives for solving various problems, by minimizing the difference between actual and predicted results. Ilkhani et al.[16] provided a relationship for estimating the shear strength of RC beam-column joints strengthened by FRP using neural networks. In 2019, Rezaie-Balf,[17] by collecting 228 experimental case studies of the scour depth downstream of sluice gates with an apron and using multivariate adaptive regression splines (MARS), proposed a relationship for the scour depth. Moodi et al.[18] used the response surface methodology (RSM) to estimate the relative bond strength of lap-spliced RC beams with both tensile and stirrup bars corrosion. Behbahani et al.[21] in 2018, proposed models based on artificial neural network (ANN) and particle swarm algorithm (PSO) for estimating driving time. They showed that the performance of ANN method was better than that of the model based on PSO algorithm. Mai et al.[24] used a new combined artificial intelligence method (RBFNN with meta-heuristic algorithms) to estimate the compressive strength of concrete-filled steel tubular (CFST). A new optimization algorithm inspired by the frefy movement (FFA) was proposed in that study. They found that the proposed model by RBFNN-FFA has the highest efficiency and accuracy for predicting the axial compression capacity of CFST compared to ANN. In another study, axial compression capacity of these columns (CSFT) was estimated by developing novel models using the Gene Expression Programing (GEP). The results showed that GEP is a powerful tool for extracting a new model with complex behavior.[25] ANN, M5 Tree (M5Tree), MARS, locally weighted polynomials (LWP), Kriging (KR), and extreme learning machines (ELMs) were used for estimating the maximum pitting corrosion depth in oil and gas pipelines by Ben Seghier et al.[26]

In previous studies, various machine learning methods have been used for estimating the compressive strength of columns confined by FRP sheets (circular and square/rectangular). Table 1 reports these studies along with the number of specimens, machine learning method, and type of cross-section (circular and rectangular). As shown in Table 1, few studies have been presented on the use of machine learning (ML) methods to estimate the compressive strength

of square/rectangular columns confined by FRP, in previous studies. In the studies of Wu et al.,[27] only the RBFNN method was used for estimating the compressive strength of square/rectangular concrete confined with FRP. Their results showed that RBFNN method is practical method for predicting this compressive strength. The type of ANN network, used in Pham and Hadi[28] study for estimating the compressive strength/strain of those columns, was feed-forward back propagation. Note that the type of FRP used in database of Pham and Hadi[28] study was only CFRP. In Doran et al.[29] study, fuzzy logic methodology was used for RC columns confined with CFRP and their database did not include FRP types. Mohana[30] used ANN and SVR methods to estimate the lateral confinement coefficient (Ks) of CFRP-confined RC columns.

Finding a method to estimate compressive strength of square/rectangular concrete columns confined with FRP, that is suitable for all types of columns (columns with different unconfined compressive strength and different types of FRP), is one of the basic needs of structural strengthening for engineers. Note that in previous studies that have used ML methods to estimate the compressive strength of those columns, the FRP type and compressive strength of unconfined concrete have been limited. For this purpose, in this study, an attempt was made to collect a comprehensive database from previous studies, as an innovation. In this study, initially, experimental data of square and rectangular concrete specimens, confined by FRP, are collected from the available papers. Note that a wider range of statistical populations leads to more reliable results for the estimation purpose. The used statistical population of this study is wider compared to the previous studies. As shown in Table 1, the largest statistical population used in previous studies for rectangular/square specimens has been 416 (Moodi et al.[12]). The database consisted of 463 specimens, 324 (70%) of which were used for modeling and 139 (30%) were employed for evaluating methods. This database includes normal strength concrete (NSC) and high strength concrete (HSC). Also, different types of FRP confinement were used in this database. Finding an accurate method for estimating the compressive strength of square/rectangular columns confined with FRP types and concrete types (NSC and HSC) is innovation of this study. Accordingly, machine learning methods were used to estimate the compressive strength of square and rectangular columns confined by various FRP sheets. The accuracy of such ML's as the multilayer perceptron (MLP) combined with Levenberg–Marquardt algorithm, radial basis functions neural networks (RBFNN), and support vector regression (SVR), used in this study, was compared with one another and with those presented in previous studies, to select the best method to estimate the compressive strength of FRP-confined columns. The results showed that MLP and RBFNN methods estimate the compressive strength of FRP-confined columns more accurately compared to the SVR method and the models of previous studies.

Some existing models of previous studies

Different models have been proposed to estimate the compressive strength of square and rectangular columns confined by FRP, in the past. Some of those are summarized in Table 2 for comparison purposes.

In the study by Lam and Teng,[7] the effective strain factor (k_ε) was defined as the ratio of the FRP actual hoop rupture strain to the ultimate tension strain of FRP materials. This factor, in their study, was considered 0.851, 0.586, 0.624, and 0.788 for AFRP, CFRP, GFRP, and HM-CFRP, respectively. In the mentioned study, the section shape factor (k_a) was related to the confined effective area and the ratio of faces (b/h). In a rectangular cross-section, only some zones were effectively confined at the cross direction. They assumed that the concrete that was confined effectively consisted of four parabolas that cut corners with 45°. In Pham and Hadi,[8] the section shape coefficient was defined as the ratio of the total length of four rounded corners (for preventing stress concentration) to the total circumference of the section. Note that in Pham and Hadi's[8] study, if the radius of the corner is zero, the confined stress $(f_{l,a})$ would be undefined and the calculation of the compressive strength of confined concrete would be impractical. Section shape coefficient in the study of Harajli et al.,[3] Ilki and Kumbasar,[4] and Toutanji et al.[10] was considered such as in the Lam and Teng[7] model.

Experimental data

Many studies have been conducted on the concrete confined by FRP. In this study, a statistical population with 463 square and rectangular concrete specimens, confined by FRP, have been extracted from references as follows: Al-Salloum,[51] Benzaid et al.,[52] Campione,[53] Compione et al.,[54] Carrazedo,[55] Chaallal et al.,[56] Demers and Neale,[57] Erdil et al.,[58] Harajili et al.,[3] Harries and Carey,[59] Hosotani et al.,[60] Ignatowski and Kaminska,[61] Ilki and Kumbasar,[4] Lam and Teng,[7] Masia et al.,[62] Mirmiran et al.,[63] Modarelli et al.,[64] Parvin and Wang,[65] Rochett and Labossiere,[66] Rousakis et al.,[67] Rousakis and Karabinis,[68] Shehata et al.,[69] Suter and Pinzelli,[70] Tao et al.,[71] Wang and Wu,[72–74] Wang et al.,[75,76] Wu and Wei,[77] Yan et al.,[78] Yeh and Chang,[79] Youssef et al.,[80] Zhang et al.,[81] Ozbakkaloglu and Oehlers,[82] Ozbakkaloglu,[83] Ozbakkaloglu,[84] Fanggi and Ozbakkaloglu,[85] Fallah Pour et al.,[86] Demir et al.,[87] and Ozbakkaloglu.[88]

The existing square and rectangular specimens of this statistical population include the width (b) of 70–450 mm, the length (h) of 7–600 mm, the corner radius (r) offset of 0–60, and the unconfined compressive strength (f_{co}) of 10–110.8 MPa. Different types of FRPs include CFRP, AFRP, and GFRP. All the FRP sheets used in these data have been

Table 2. Some of available models for compressive strength prediction of FRP-confined rectangular and square concrete columns.

Reference	Model	Description
Moodi et al.[11]	$f'_{cc} = f'_c\left(1 + 3.3k_\varepsilon \frac{f_{l,a}}{f'_c}\right)$	$f_{l,a} = \frac{2E_{frp}t_j\varepsilon_{frp}}{D}$ $k_\varepsilon = \frac{\pi r + 0.1996b + 0.0107h}{b + h - (4-\pi)r}, \quad D = \sqrt{b^2+h^2}$
Harajli et al.[3]	$f'_{cc} = f'_c\left(1 + 1.25\sqrt{\frac{k_a\rho_f E_{frp}\varepsilon_{fe}}{2f'_c}}\right)$	$k_a = 1 - \frac{(b-2r)^2 + (h-2r)^2}{3bh}$ $\rho_f = \frac{4t_j}{D}, \; D = \frac{2bh}{b+h}$
Ilki and Kumbasar[4]	$f'_{cc} = f'_c(0.6{+}0.2\frac{b}{h})(1{+}2.29\left(\frac{f_{l,a}}{f'_c}\right)^{0.87})$	$f_{l,a} = \frac{k_a\rho_f F_{frp}}{2}, \; \rho_f = \frac{2t_j(b+h)}{bh}$ $k_a = 1 - \frac{(b-2r)^2 + (h-2r)^2}{3bh} - \frac{(4-\pi)r^2}{bh}$
Lam and Teng[7]	$f'_{cc} = f'_{co}\left(1 + 3.3k_a\frac{f_{l,a}}{f'_{co}}\right)$	$f_{l,a} = \frac{2E_{frp}t_j\varepsilon_{h,rup}}{D}$ $\varepsilon_{h,rup} = k_\varepsilon\varepsilon_{frp}, \quad D = \sqrt{b^2+h^2}$ $k_a = \left(\frac{b}{h}\right)^2\left[1 - \frac{\left(\frac{b}{h}\right)(h-2r)^2 + \left(\frac{h}{b}\right)(b-2r)^2}{3A_g}\right]$
Pham and Hadi[8]	$f'_{cc} = f'_{co}\left(0.68 + 3.91k_a\frac{f_{l,a}}{f'_{co}}\right)$	$f_{l,a} = \frac{E_{frp}t_j\varepsilon_{h,rup}}{r}$ $k_\varepsilon = 0.5 + 0.642\ln(A)$ $A = \frac{2r}{bR_s}, \quad R_s = \frac{t_jE_{frp}}{\left(\frac{f'_{co}}{\varepsilon_{co}}\right)r}$ $\varepsilon_{co} = (-0.067f'^2_{co} + 29.9f'_{co} + 1053)10^{-6}$
Wei and Wu[9]	$f'_{cc} = f'_c(1{+}2.2\left(\frac{2r}{b}\right)^{0.72}\left(\frac{f_{l,a}}{f'_c}\right)^{0.72}\left(\frac{h}{b}\right)^{-1.9}$	$k_\varepsilon = \frac{\pi r}{b + h - (4-\pi)r}$ $f_{l,a} = \frac{2F_{frp}t_j}{b}$
Toutanji et al[10]	$f'_{cc} = f'_c + 4\left(\frac{2r}{D}\right)^{0.1}\left(\frac{h}{b}\right)^{0.13}k_af_{l,a}$	$f_{l,a} = \frac{2E_{frp}\varepsilon_{fe}t_j}{D}, \; D = \frac{2bh}{h+b}$ $k_a = 1 - \frac{(b-2r)^2 + (h-2r)^2}{3bh}$

one-direct (hoop direction). Monotonic loading has been applied for the specimens utilized in this database. Experimental specimen details are shown in Table 3. Among these specimens, 324 have been used for modeling (instructor specimens) with 139 selected for evaluation (appraiser specimens) randomly.

Machine learning methods for estimation

Due to their quick learnability and good output accuracy, ML is among the very efficient methods for different estimation cases. In general, ANN methods are inspired by the human brain's neural system and its processing units, which are called neurons, to classify complex data and predict events' behavior intelligently. In 1943, McCulloch and Pitts[89] designed the first artificial neuron that could, as its main feature, yield an output of 0 or 1, if all the weighted input signals were respectively less or greater than a certain threshold. In the late 1950s, Rosenblatt et al.[90] introduced the Perceptron Neural Networks where the neurons were similar to those designed by McCulloch and Pitts, but

Table 3. The collected experimental specimen details for proposing the model.

Number	Reference	Specimen number	Fiber type	B (mm)	H (mm)	r (mm)	fc (MPa)
1	Al-Salloum[51]	8	CFRP	150	150	5–50	26.7–31.8
2	Benzaid et al.[52]	6	GFRP	100	100	0–16	54.8
3	Campione[53]	2	CFRP	150	150	3	13
4	Campione et al.[54]	1	CFRP	152	152	3	20.1
5	Carrazedo[55]	4	CFRP	150	150	10–30	33.5–36.5
6	Chaallal et al.[56]	24	CFRP	95.25–133.35	133.35–190.5	25.4	21.4–55.4
7	Demers and Neale[57]	5	CFRP, GFRP	152	152	5	32.3–42.2
8	Erdil et al.[58]	1	CFRP	150	150	25	10
9	Harajili et al.[3]	9	CFRP	79–132	132–214	15	18.9–21.5
10	Harries and Carey[59]	4	GFRP	152	152	11–25	31.2–32.4
11	Hosotani et al.[60]	4	CFRP, HM-CFRP	200	200	30	38.1
12	Ignatowski and Kaminska[61]	3	CFRP	100–105	100–200	10	32.3
13	Ilki and Kumbasar[4]	12	CFRP	150–250	250–300	40	32.8–34
14	Lam and Teng[7]	12	CFRP	150	150–225	15–25	24–41.5
15	Masia et al.[62]	15	CFRP	100–150	100–150	25	21.3–25.7
16	Mirmiran et al.[63]	9	CFRP	152.5	152.5	6.35	40.6
17	Modarelli et al.[64]	6	CFRP, GFRP	150	150–200	10–25	17.6–25
18	Parvin and Wang[65]	2	CFRP	108	108	8.26	22.6
19	Rochett and Labossiere[66]	26	CFRP, AFRP	152	152–203	5–38	35.8–43.9
20	Rousakis et al[67]	15	CFRP, GFRP	200	200	30	33–39.9
21	Rousakis and Karabinis[68]	4	CFRP, GFRP	200	200	30	25.5
22	Shehata et al[69]	8	CFRP	94–150	150–188	10	23.7–29.5
23	Suter and Pinzelli[70]	16	CFRP, GFRP, AFRP, HM-CFRP	150	150	5–25	33.9–36.7
24	Tao et al.[71]	24	CFRP	150	150–300	20–50	19.5–49.5
25	Wang and Wu[72]	60	CFRP	150	150	0–60	29.3–55.2
26	Wang and Wu[73]	9	AFRP	100	100	10	46.4–101.2
27	Wang and Wu[74]	15	AFRP	70–150	70–150	7–15	34.6–52.1
28	Wang et al.[75]	10	CFRP	100–400	100–400	10–45	24.4
29	Wang et al.[76]	8	CFRP	204–305	204–305	20–30	25.5
30	Wu and Wei[77]	30	CFRP	150	150–300	30	32.3–42.4
31	Yan et al.[78]	2	CFRP, GFRP	279	279	19	15.2
32	Yeh and Chang[79]	28	CFRP	150–450	150–600	30	20.6
33	Youssef et al.[80]	37	CFRP, GFRP	254–381	381	38	29.2–38.7
34	Zhang et al.[81]	2	AFRP	150	150	15	45–50
35	Ozbakkaloglu and Oehlers[82]	6	CFRP	150–200	200–300	10–40	24–26.7
36	Ozbakkaloglu[83]	11	CFRP	112.5–150	150–225	15–30	107.3–110.8
37	Ozbakkaloglu[84]	19	CFRP	112.5–150	150–225	15–30	76.6–79.6
38	Fanggi and Ozbakkaloglu[85]	2	AFRP	150	150	30	98.2
39	Fallah Pour et al.[86]	2	CFRP	150	150	30	104.8
40	Demir et al.[87]	3	CFRP	150	150–225	25	93.8–106
41	Ozbakkaloglu[88]	4	CFRP	112.5–150	150–225	15–30	107.8

different in training rules to solve pattern recognition problems as perceptron networks were unable to implement a series of specific basic functions.[91] Finally, multi-layer perceptron networks and their related learning rules introduced in the late 1980s overcame these limitations.[92]

In this study, MLP, RBFNN, and SVR methods were used to estimate the compressive strength of square and rectangular columns confined by FRP. Those methods have been introduced in the following sections.

Multilayer perceptron (MLP) artificial neural networks

The multilayer perceptron is a very powerful and widely used ANN with generally three input, hidden, and output

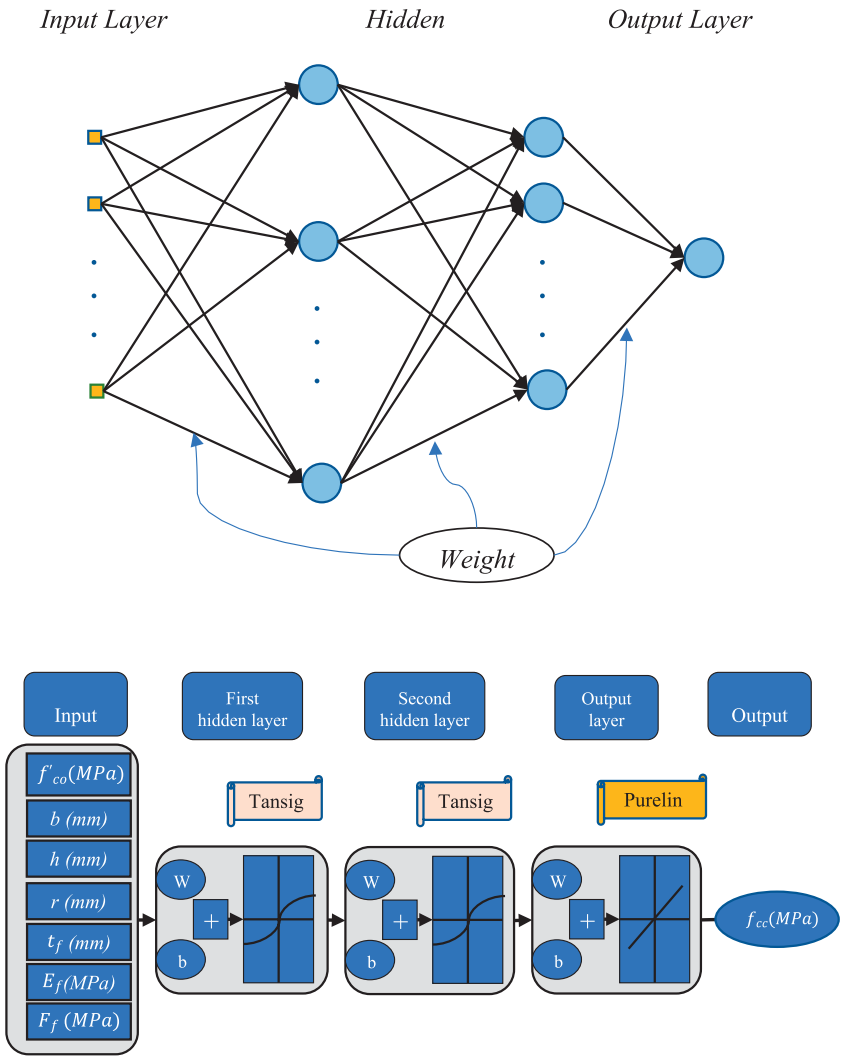

Figure 1. Basic schematic and proposed MLP network for prediction of f_{cc}.

layers; the input layer is generally a part of the hidden layer and the latter, with several layers,[93] is, indeed, the central core of the input processing which eventually transfers them to the output layer.

Each layer has a different number of neurons linked together with weights based on their values to which another component called "bias" is added.[94] The output of MLP can be explained as follows

$$y_j = \mathrm{g}\left(\sum_{i=1}^{M} w_{ij}x_{ij} + b_j\right) \quad (1)$$

Here, w_{ij} and x_{ij} represent the weight and input from i^{th} neuron in the previous layer to j^{th} neuron in the current layer, respectively. b_j signifies the bias associated with the j^{th} neuron.

This layer-to-layer data-transfer is through "transfer functions" (g ()) also known as "activation functions" among which Tansig and Logsig (both subsets of sigmoid functions) are widely used for hidden layers, while the Pureline, defined as follows, is used for the output layer[95]

$$\text{Logsig} \ : \ \mathrm{g(x)} = \frac{1}{1+\mathrm{e}^{\mathrm{x}}} \quad (2)$$

$$\text{Tansig} \ : \ \mathrm{g(x)} = \frac{\mathrm{e}^{\mathrm{x}} - \mathrm{e}^{-\mathrm{x}}}{\mathrm{e}^{\mathrm{x}} + \mathrm{e}^{-\mathrm{x}}} \quad (3)$$

$$\text{Pureline} \ : \ \mathrm{g(x)} = \mathrm{x} \quad (4)$$

During the training process of MLP, the learning algorithm adjusts weights and bias values to minimize the error between the actual and predicted data.[95,96] Numerous learning algorithms such as scaled conjugate gradient (SCG), Cartesian genetic programming (CGP), Broyden–Fletcher–Goldfarb–Shanno (BFGS), and Levenberg–Marquardt (LM) are commonly used in learning, the most common of which is the LM algorithm[96] whose architecture is displayed in Figure 1.

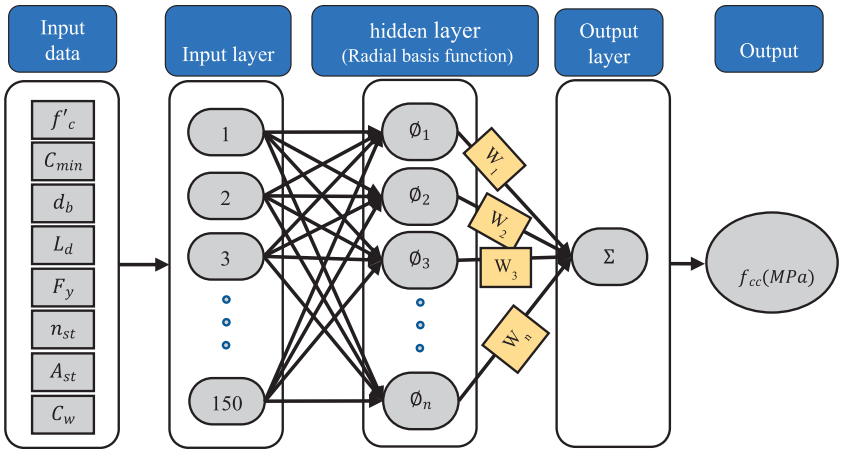

Figure 2. Structure of RBFNN.[100]

Radial basis function neural networks (RBFNNs)

RBFs are forward propagation networks, in whose hidden layer, the radial basis function is used as the activation function. The RBF network estimates each function, using symmetric and local radial functions.[97]

As with MLP networks, RBF networks also consist of input, hidden, and output layers with the difference that the hidden layer has only one layer. "Gaussian," is the most widely used basic function used in RBF networks comparable to linear, polynomial, spline, and multi-degree inverse functions.

In this network, input variables are given to the network in the form of a vector and are subjected to a nonlinear transformation in the hidden layer. This suggests that the RBFNN activation function in the hidden layer serves as network neurons. Before applying a nonlinear change by the RBFNN activation function, the input variables must be multiplied by the corresponding bias. A vector whose difference between the multiplied inputs and their associated weights is given as the input of the RBF activation function.[98] The network output for an input pattern, such as x, can be expressed as Equation (5)

$$y(x) = \sum_{k=1}^{J_2} w_k \varphi(||x - c_k||) \tag{5}$$

where y denotes the RBFNN output, w_k represents the weight of the k connection of the hidden layer neuron to the output, and ||.|| and ∅ (0) show the Euclidean rule and the Gaussian function, respectively. The Gaussian function is defined as follows[99]

$$\varphi(d) = \exp\left(\frac{d^2}{2\sigma^2}\right) \tag{6}$$

where φ is the Gaussian function, σ^2 is the spread coefficient, and d represents the Euclidean distance expressed as follows

$$d_i = \sqrt{\sum_{k=1}^{m} (X_k - C_{ki})^2} \tag{7}$$

where m and C_{ki} are the number of variables and centers, respectively. Figure 2 displays the RBFNN structure for a better understanding.

Support vector regression (SVR)

Support vector machines (SVMs) are, in fact, a subset of machine learning techniques that lie in the supervised learning category and are often used in classification, regression, and prediction problems. As with ANN, SVM is a data-driven algorithm that, unlike ANN's that may sometimes converge in local responses, establishes a connection between the input data and the target-dependent variable, based on the structural risk minimization.[101,102] Being based on the statistical learning theory, it considers the operational risk as a target function and pursues the optimal solution instead of reducing the computational error.[103,104] It was developed by Vapnik in the mid-1990s[105] as it could solve complex structure problems, predict with minimal error, and provide the general optimal response.

Assuming one dataset, infinite lines, planes, and hyperplanes can be considered as separators in 2D, 3D, and mD spaces, respectively, to divide the data into two classes.[106] Any datum the least far from these lines, planes, or hyperplanes is called a support vector; the farther are the two, the more optimum is the separating member. As mentioned, one of the applications of SVMs is regression, hence the name support vector regression (SVR).[102] In

SVMs, mapping is used to transfer data from an mD space to a higher dimensional feature space with separable linear output data. The equation of this hyperplane can be expressed as follows

$$f(x) = W^T X + b \tag{8}$$

where W is an mD vector to determine the direction of the hyperplane and b is the bias component. The objective is to find the optimal value of the hyperplane, which, as mentioned, should be the farthest from the support vectors. To this end, it can be expressed, based on mathematical calculations, as follows[107]

$$\text{Minimize } \frac{1}{2}\|W\|^2$$
$$\textit{Subject to} \begin{cases} Y_i\text{-}W^T X_i - b \le \varepsilon \\ W^T X_i + b\text{-}Y_i \le \varepsilon \end{cases} \tag{9}$$

In some cases, the data may lie outside their specified class borders and enter another class. Assuming ξ^+ and ξ^- as the violation from one class to another which is called slack variables, equation (10) can be rewritten as follows

$$\text{Minimize } \frac{1}{2}\|W\|^2 + C\sum_{i=1}^{l}\left(\xi_i^+ + \xi_i^-\right)$$
$$\text{Subject to} \begin{cases} Y_i - W^T X_i - b \le \varepsilon + \xi_i^- \\ W^T X_i + b - Y_i \le \varepsilon + \xi_i^+ \\ \xi_i^-, \xi_i^+ \ge 0 \end{cases} \tag{10}$$

where C indeed plays the role of a regularization factor for the data violating the threshold (ε). In cases where the data are linearly inseparable, an auxiliary tool is used in the hyperplane equation (assuming an mD data space) to enable their mapping in a linear space; this process is called the kernel trick,[105] whose usage enables the data to be mapped from a nonlinear to linear space for becoming separable. The hyperplane equation is thus expressed as follows

$$W^T X + b = 0 \rightarrow W^T \phi(X) + b = 0 \tag{11}$$

where ∅ is the kernel function (expressed also as K (x_i, x_j)) responsible for mapping from nonlinear to linear space. Nowadays, various functions, such as linear, polynomial, sigmoid, and Gaussian, are used as kernel functions, among which the Gaussian with the following equation is used more due to its high computational efficiency and special performance[107]

$$K(X_i, X_j) = \exp\left(-\gamma \|X_i - X_j\|^2\right) \tag{12}$$

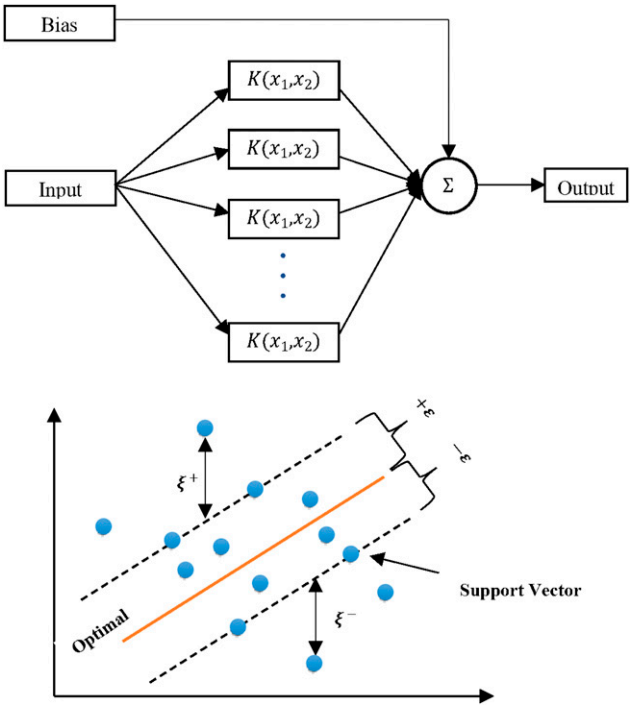

Figure 3. Flowchart and schematic of a typical support vector regression.

where γ, a kernel function parameter, shows the spatial distribution. Figure 3 depicts the flowchart and a schematic view of the SVR method.

Method setting parameters

Artificial neural networks contain several regulatory parameters, whose optimal determination will contribute to the best network performance; the number of layers, the number of neurons in each layer, and transfer functions of each layer are the regulatory parameters in MLP networks. For estimating the compressive strength of square and rectangular columns confined by FRP, this study has used a 150-run trial and error method plus a 3-layer perceptron ANN with one output layer and two hidden layers with Pureline and Tansig activation functions, respectively, along with the Levenberg–Marquardt training algorithm and back propagation error technique. In RBF networks, where the number of neurons and training function are considered two parameters, "spread" is a parameter that indicates the extension of the radial functions. This means that the more scattered the data are, the larger the "spread" should be. Via trial and error, an RBF ANN has been used for this study with the Gaussian as its basic function with 150 neurons and a spread of 499. In SVR, parameters such as the allowable violation from the

Table 4. Statistical indicators related to previous studies models.

Model	MSE	AAE	SD	e_{tot}	R^2
Moodi et al.[11]	**2.43**	**12.15**	**15.59**	**12.91**	**0.87**
Wei and Wu[9]	**3.73**	**14.90**	**18.74**	**16.51**	**0.86**
Toutanji et al.[10]	6.44	18.60	23.23	20.67	0.82
Pham and Hadi[8]	11.35	23.99	32.05	25.44	0.75
Harajli et al.[3]	9.82	26.02	23.47	27.17	0.81
Ilki and Kumbasar[4]	6.90	18.62	25.99	20.24	0.79
Lam and Teng[7]	5.27	16.11	22.63	16.86	0.82

Table 5. Statistical indicators related to LM methods.

	Methods	MSE	AAE	SD	e_{tot}	R^2
Training	MLP	0.67	5.66	8.19	6.12	0.98
	RBFNN	0.30	3.74	5.45	4.43	0.99
	SVR	2.06	9.61	14.35	11.25	0.92
Test	MLP	1.52	8.33	12.27	7.60	0.94
	RBFNN	1.58	8.48	12.42	7.73	0.93
	SVR	4.21	13.93	20.15	12.36	0.86

class borders, penalty coefficient, type, and the kernel function parameters play important roles in achieving the optimal solution. This study has used SVR with a regularization factor = 0.89, slack variable = 0.015, and Gaussian kernel function.

Results and discussion

In this section, the performance of previous study models as well as the machine learning methods used in this study to estimate the compressive strength of square plus rectangular columns confined by FRP are compared and discussed. For this purpose, first, the models of previous studies were compared with each other where two models with more accuracy were selected. Accordingly, machine learning methods were more accurately compared with each other and with the models. To evaluate their performance, widely used indicators have been used including standard deviation (*SD*), mean squared error (*MSE*), absolute integral error (*IAE*), and total error (e_{Total}). Their related equations are (13) to (16), respectively, as follows

$$\mathrm{MSE} = \frac{\sum_1^N \left(\frac{\mathrm{Theo_i}-\mathrm{Expe_i}}{\mathrm{Expe_i}}\right)^2}{\mathrm{N}} \tag{13}$$

$$\mathrm{AAE} = \frac{\sum_1^N \left|\frac{\mathrm{Theo_i}-\mathrm{Expe_i}}{\mathrm{Expe_i}}\right|}{\mathrm{N}} \tag{14}$$

$$\mathrm{SD} = \sqrt{\frac{\sum_1^N \left(\frac{\mathrm{Theo_i}}{\mathrm{Expe_i}} - \frac{\mathrm{Theo_{avg}}}{\mathrm{Expe_{avg}}}\right)^2}{\mathrm{N\text{-}1}}} \tag{15}$$

$$\mathrm{e_{tot}} = \frac{\sum_1^N |\mathrm{Expe_i}-\mathrm{Theo_i}|}{\sum_1^N |\mathrm{Expe_i}|} \tag{16}$$

where N is the number of specimens and Exp_i and $Theo_i$ are, respectively, the experimental compressive strength of square and rectangular columns confined by FRP and those predicted by machine learning or models of previous studies.

Table 6. Statistical parameters for confined concrete specimens with FRP.

Model	MSE	AAE	SD	e_{tot}
Moodi et al[11]	2.43	12.15	15.59	12.91
Wei and Wu[9]	3.73	14.90	18.74	16.51
MLP	0.92	6.46	9.63	5.75
RBFNN	0.68	5.16	8.25	4.84
SVR	2.71	10.91	16.33	10.09

Performance evaluation of the previous studies models

The models presented in previous studies are compared based on the total specimens as these models are not presented based on the specimens of this study. To compare the models, statistical indices were calculated based on the total specimens in Table 3 and presented in Table 4.

As reported in Table 4, statistical indicators related to Moodi et al.[11] and Wei and Wu[9] models are the lowest values in comparison with other models. The total error of Moodi et al.[11] as well as Wei and Wu[9] models are by average 42 and 25%, respectively, less than other models (Toutanji et al.,[10] Pham and Hadi,[8] Harajli et al.,[3] Ilki and Kumbasar,[4] and Lam and Teng[7]). Hence, these two methods were selected as the best methods for estimating the compressive strength of square and rectangular columns confined by FRP.

Performance evaluation of the proposed LM methods

To evaluate the LM methods' performance, statistical indices were calculated for training and test specimens, separately, as presented in Table 5. Those methods were compared based on statistical indices of test specimens. The results of Table 5 indicate that LM methods have performed well in estimating the compressive strength of square and rectangular FRP-confined columns.

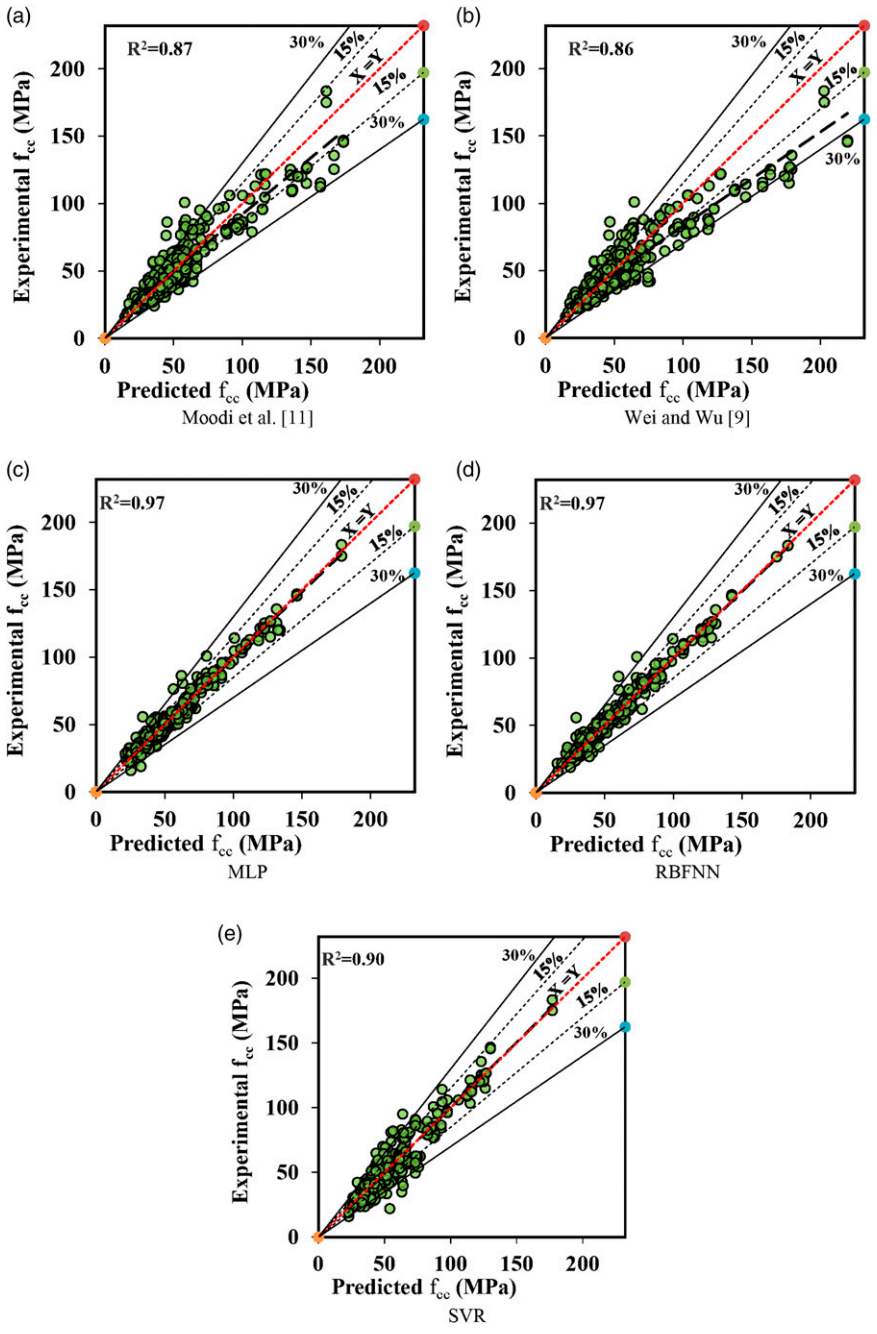

Figure 4. Performance of models.

According to Table 5, MLP and RBFNN methods have had a close performance, and for training and test specimens, they have outperformed the SVR method. The average statistical indices of MLP and RBFNN methods have been 0.59 and 0.6 time that of SVR method in test specimens, respectively. Note that the difference between training statistical indicators and test ones has been high in the RBFNN method, with this difference indicating the poor performance of RBFNN. Thus, the MLP method can be selected as the best LM method for estimating the compressive strength of square and rectangular FRP-confined columns.

Comparison of LM methods and the models of previous studies

To compare the performance of LM methods with two best models of previous studies (Moodi et al.[11] and Wei and Wu[9]), statistical indices of total specimens are presented in Table 6.

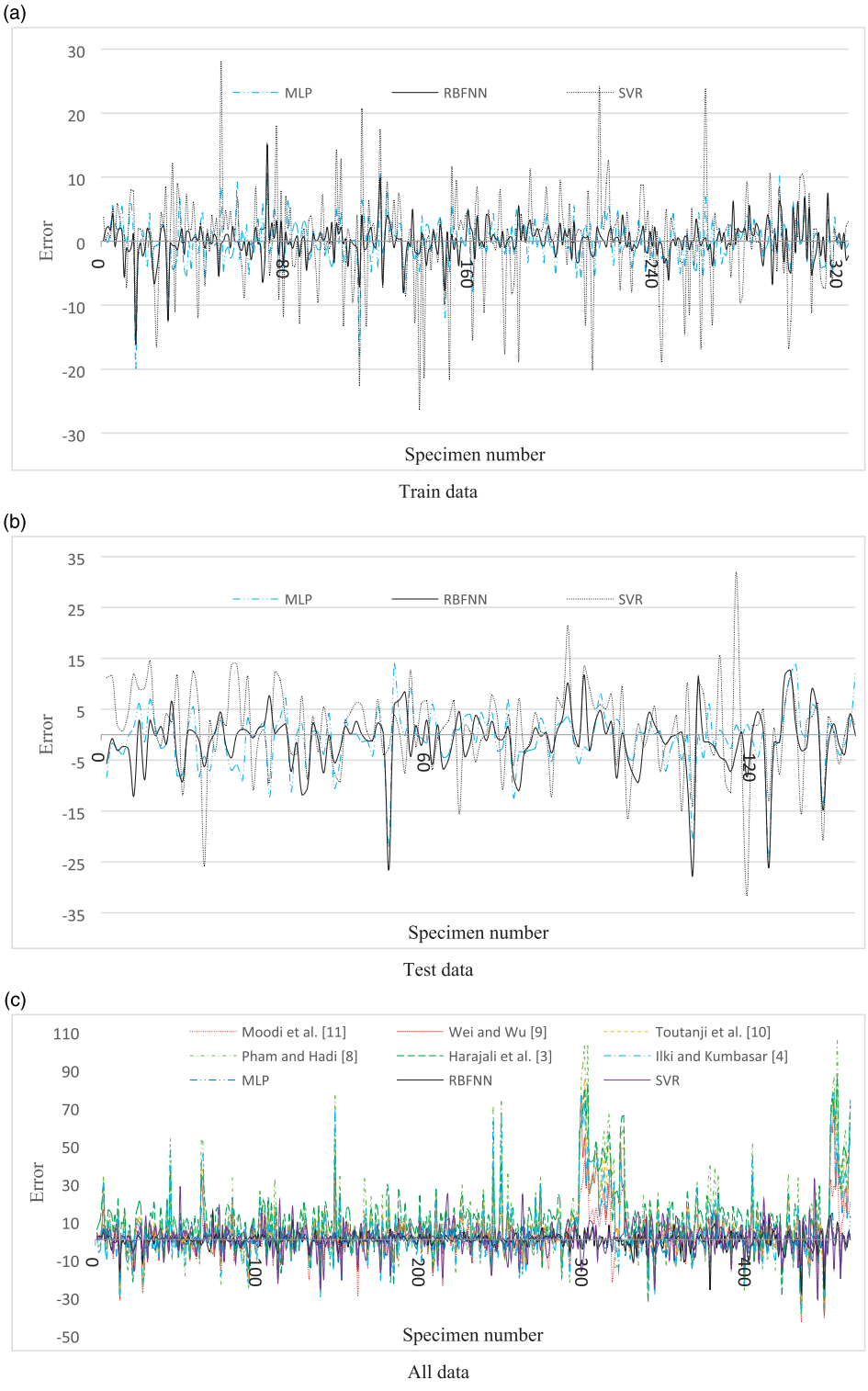

Figure 5. Comparison of performance for experimental data.

As shown in Table 6, the differences between the statistical indicators of MLP and RBFNN methods and the models of previous studies were significant, but those of the SVR method were close to Moodi et al.[11] and Wei and Wu[9] models.

To illustrate the efficiency of LM and the models of previous studies, experimental compressive strength against compressive strength resulting from MLP, RBFNN, and SVR methods and Moodi et al.[11] and Wei and Wu[9] is

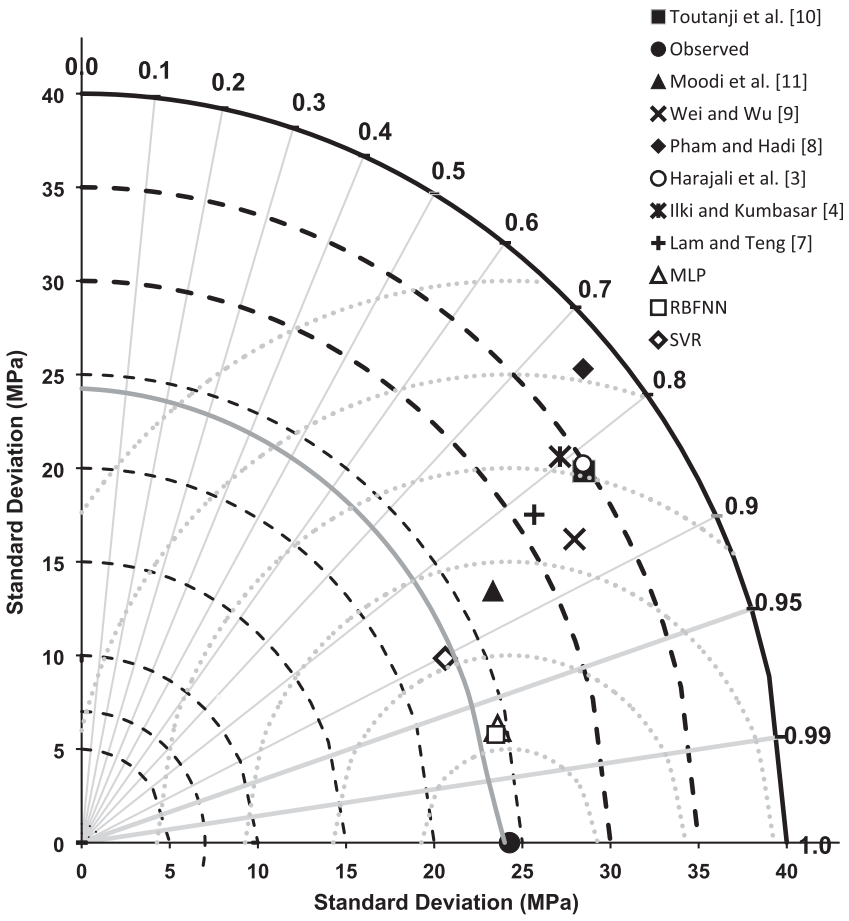

Figure 6. Taylor diagram plots of the ML methods and the models of previous studies for all specimens.

outlined in Figures 4(A) to (E). Among LM methods and the models of previous studies, LM methods have had a higher correlation coefficient (R^2). Among the LM methods, the correlation coefficient of RBF and MLP methods has been the highest.

Figure 5 shows that the error values obtained from LM methods are acceptable and can estimate the values of the strength of the rectangular and square columns confined by FRP.

Taylor diagram

Finally, in order to determine the accuracy of the best or worst method/model, Taylor diagram was used. In past studies, this diagram has been used to compare estimating methods.[108,109] This type of diagram combines several indices in order to present how the predicted values are matched against the real measurements. Using three error criteria, standard deviation, correlation coefficient, and RMSE, Taylor diagram was plotted for the total specimens as displayed in Figure 6. Note that any method closer to the observed point has greater accuracy for estimating the compressive strength of FRP-confined column. It can be seen that the RBFNN method is the closest to the observed result circle, followed by the MLP and SVR, but RBFNN and MLP methods are close to each other. Only in the SVR method, the division standard has been smaller than the observed value and this method has the closest value of division standard to the observed. Among the models of previous studies, the model of Moodi et al.[11] has been closer to the actual observed value.

Conclusion

Estimation of compressive strength of concrete confined with FRP, that is suitable for all types of columns, is one of the basic needs of structural strengthening for engineers. In this paper, three machine learning methods were used to predict the compressive strength of the square and rectangular concrete columns confined with FRP types and concrete types (NSC and HSC). These methods included MLP, RBFNN, and SVR. Finding a suitable method for all types of concrete and FRP confinement has been the novelty of this study. To train and evaluate these methods, a comprehensive database, containing 463 specimens of FRP-confined rectangular/square concrete, was used. These

machine learning methods were compared with each other as well as with the models of previous studies, with the following results obtained:

1 Among the models of previous studies, Moodi et al.[11] and Wei and Wu[9] models had a better performance for estimating the compressive strength of FRP-confined square/rectangular concrete columns, with the correlation coefficient of these models being 0.87 and 0.86, respectively.
2 All three machine learning methods for estimating the compressive strength of FRP-confined square/rectangular concrete columns were more accurate than the models of previous studies.
3 Among the methods of ML used in this study, MLP and RBFNN methods have better performance rather than the SVR method.
4 The difference between training statistical indicators and the test ones was high in the RBFNN method, with this difference reflecting the poor performance of RBFNN compared to MLP methods.

Nevertheless, more detailed studies are required for estimating the compressive strength of the square and rectangular concrete columns confined with FRP. The use of hybrid soft computational approaches (ANN methods with optimization algorithms) or new methods such as high correlated variables creator machine, multiple Ln equation regression, and genetic programming can be recommended for estimating this strength in future studies.

Declaration of conflicting interests

The author(s) declared no potential conflicts of interest with respect to the research, authorship, and/or publication of this article.

Funding

The author(s) disclosed receipt of the following financial support for the research, authorship, and/or publication of this article: This work was supported by the University Of Velayat (grant no: P-99-1-32).

ORCID iDs

Yaser Moodi https://orcid.org/0000-0002-3763-1629
Mohammad Ghasemi https://orcid.org/0000-0002-4692-7392

References

1. Ahmad SH, Khaloot AR and Irshaid A. Behaviour of concrete spirally confined by fibreglass filaments. *Mag Concr Res* 1991; 43(156): 143–148. DOI: 10.1680/macr.1991.43.156.143.
2. Nanni A and Bradford NM. FRP jacketed concrete under uniaxial compression. *Constr Build Mater* 1995; 9(2): 115–124. DOI: 10.1016/0950-0618(95)00004-Y.
3. Harajli MH, Hantouche EG and Soudki K. Stress-strain model for fiber-reinforced polymer jacketed concrete columns. *ACI Struct J* 2006; 103(5): 672–682, Accessed: Apr. 30, 2021. [Online]. Available:, https://www.concrete.org/restrictedcountry.aspx.
4. Ilki A and Kumbasar N. Compressive behaviour of carbon fibre composite jacketed concrete with circular and non-circular cross-sections. *J Earthq Eng* 2003; 7(3): 381–406. DOI: 10.1080/13632460309350455.
5. Kamgar R, Naderpour H, Komeleh HE, et al. *applied Sciences A Proposed Soft Computing Model for Ultimate Strength Estimation of FRP-Confined Concrete Cylinders*.
6. Abbaszadeh MA and Sharbatdar M, Modeling of confined circular concrete columns wrapped by fiber reinforced polymer using artificial neural network. *J Soft Comput Civ Eng* 2020; 4(4); 61–78. doi: 10.22115/SCCE.2020.213196.1153.
7. Lam L and Teng JG. Design-oriented stress-strain model for frp-confined concrete in rectangular columns. *J Reinf Plast Compos* 2003; 22(13): 1149–1186. DOI: 10.1177/0731684403035429.
8. Pham TM and Hadi MNS. Stress prediction model for FRP confined rectangular concrete columns with rounded corners. *J Compos Constr* 2014; 18(1): 04013019. DOI: 10.1061/(asce)cc.1943-5614.0000407.
9. Wei YY and Wu YF. Unified stress-strain model of concrete for FRP-confined columns. *Constr Build Mater* 2012; 26(1): 381–392. DOI: 10.1016/j.conbuildmat.2011.06.037.
10. Toutanji H, Han M, Gilbert J, et al. Behavior of large-scale rectangular columns confined with FRP composites. *J Compos Constr* 2010; 14(1): 62–71. DOI: 10.1061/(asce)cc.1943-5614.0000051.
11. Moodi Y., Farahi Shahri S and Mousavi SR. Providing a model for estimating the compressive strength of square and rectangular columns confined with a variety of fibre-reinforced polymer sheets. *J Reinf Plast Compos* 2017; 36(21): 1602–1612. DOI: 10.1177/0731684417720837.
12. Moodi Y, Mousavi SR, Ghavidel A, et al. Using response surface methodology and providing a modified model using whale algorithm for estimating the compressive strength of columns confined with FRP sheets. *Constr Build Mater* 2018; 183: 163–170. DOI: 10.1016/j.conbuildmat.2018.06.081.
13. Moodi Y, Mousavi SR and Sohrabi MR. New models for estimating compressive strength of concrete confined with FRP sheets in circular sections. *J Reinf Plast Compos* 2019; 38(21–22): 1014–1028. DOI: 10.1177/0731684419858708.
14. Naderpour H and Mirrashid M. Confinement coefficient predictive modeling of FRP-confined RC columns. *Adv Civ Eng Mater* 2020; 9(1): 20190145. DOI: 10.1520/ACEM20190145.
15. Ghasemi H, Reza M and Yaser S. "Proposing models for estimating the compressive strength of HSC and UHSC FRP - confined circular concrete by using whale algorithm," *Iran. J Sci Technol Trans Civ Eng* 2021: 0123456789. DOI: 10.1007/s40996-021-00655-2.
16. Ilkhani MH, Naderpour H and Kheyroddin A. Soft computing-based approach for capacity prediction of FRP-strengthened RC joints. *Sci Iran* 2019; 26(5 A): 2678–2688. DOI: 10.24200/sci.2018.20177.
17. Rezaie-Balf M. "Multivariate adaptive regression splines model for prediction of local scour depth downstream of an apron under 2D horizontal jets," *Iran. J Sci Technol - Trans Civ Eng* 2019; 43: 103–115. DOI: 10.1007/s40996-018-0151-y.

18. Moodi Y, Sohrabi MR and Mousavi SR. Corrosion effect of the main rebar and stirrups on the bond strength of RC beams. *Structures* 2021; 32: 1444–1454. DOI: 10.1016/j.istruc.2021.03.096.
19. Ahmadi M, Naderpour H and Kheyroddin A. ANN model for predicting the compressive strength of circular steel-confined concrete. *Int J Civ Eng* 2017; 15(2): 213–221. DOI: 10.1007/s40999-016-0096-0.
20. Azimi P and Soofi P. An ANN-based optimization model for facility layout problem using simulation technique. *Sci Iran* 2017; 24(1): 364–377. DOI: 10.24200/sci.2017.4040.
21. Behbahani H, Hosseini SM, Samerei SA, et al. "Driving time prediction at freeway interchanges using artificial neural network and particle swarm optimization," *Iran. J Sci Technol - Trans Civ Eng* 2020; 44(3): 975–989. DOI: 10.1007/s40996-019-00289-5.
22. Rakhshanimehr M, Mousavi SR, Esfahani MR, et al. Establishment and experimental validation of an updated predictive equation for the development and lap-spliced length of GFRP bars in concrete. *Mater Struct* 2018; 51(1): 1–17. DOI: 10.1617/S11527-018-1137-8.
23. Shahri SF and Mousavi SR. Bond strength prediction of spliced GFRP bars in concrete beams using soft computing methods. *Comput Concr* 2021; 24(4): 305–317. DOI: 10.12989/cac.2021.4.27.305.
24. Mai SH, Ben Seghier MEA, Nguyen PL, et al. A hybrid model for predicting the axial compression capacity of square concrete-filled steel tubular columns. *Eng Comput* 2020: 0123456789. DOI: 10.1007/s00366-020-01104-w.
25. Ben Seghier MEA, Gao XZ, Jafari-Asl J, et al. Modeling the nonlinear behavior of ACC for SCFST columns using experimental-data and a novel evolutionary-algorithm 2021; 30: 692–709. DOI: 10.1016/j.istruc.2021.01.036.*Structures*
26. Ben Seghier MEA, Keshtegar B, Taleb-Berrouane M, et al. Advanced intelligence frameworks for predicting maximum pitting corrosion depth in oil and gas pipelines. *Process Saf Environ Prot* 2021; 147: 818–833. DOI: 10.1016/j.psep.2021.01.008.
27. Jin WY, Ting GD, and Dong M, "Modeling confinement efficiency of FRP-confined concrete column using radial basis function neural network," no. 50621062, 2010.
28. Pham TM, Asce SM, Hadi MNS, et al. Predicting stress and strain of FRP-confined square/rectangular columns using artificial neural networks. *J Composites Construction* 2014; 18(6): 04014019. DOI: 10.1061/(ASCE)CC.1943-5614.0000477.
29. Doran B, Yetilmezsoy K and Murtazaoglu S. Application of fuzzy logic approach in predicting the lateral confinement coefficient for RC columns wrapped with CFRP. *Eng Struct* 2015; 88: 74–91. DOI: 10.1016/j.engstruct.2015.01.039.
30. Mohana MH, Reinforced concrete confinement coefficient estimation using soft computing models. *Period Eng Nat Sci* 2019; 7(4): 1833–1844.
31. Cevik A and Cabalar AF. A Genetic – Programming – Based Formulation for the Strength Enhancement of Fiber – Reinforced – Polymer – Confined Concrete Cylinders, 2008. DOI: 10.1002/app.
32. Cevik A and Guzelbey HI. Neural network modeling of strength enhancement for CFRP confined concrete cylinders. *Build Environ* 2008; 43: 751–763, doi:10.1016/j.buildenv.2007.01.036.
33. Hossein A, Amir G and Alavi H. New formulation for compressive strength of CFRP confined concrete cylinders using linear genetic programming. *Mater Struct*, 2010, pp. 963–983. DOI: 10.1617/s11527-009-9559-y.
34. Naderpour H, Kheyroddin A and Amiri GG. Prediction of FRP-confined compressive strength of concrete using artificial neural networks. *Compos Struct* 2010; 92(12): 2817–2829. DOI: 10.1016/j.compstruct.2010.04.008.
35. Cevik A, Gög MT, Güzelbey H, et al. Advances in engineering software soft computing based formulation for strength enhancement of CFRP confined concrete cylinders. *J.advengsoft Vol* 2010; 41: 527–536. DOI: 10.1016/j.advengsoft.2009.10.015.
36. Cevik A. Expert systems with applications modeling strength enhancement of FRP confined concrete cylinders using soft computing. *Expert Syst Appl* 2011; 38(5): 5662–5673. DOI: 10.1016/j.eswa.2010.10.069.
37. Elsanadedy HM, Abbas H and Alsayed SH. Composites: Part B prediction of strength parameters of FRP-confined concrete. *Compos B* 2012; 43(2): 228–239. DOI: 10.1016/j.compositesb.2011.08.043.
38. Jalal M and Ramezanianpour AA. "Composites: Part B strength enhancement modeling of concrete cylinders confined with CFRP composites using artificial neural networks. *Compos Part B* 2012; 43(8): 2990–3000. DOI: 10.1016/j.compositesb.2012.05.044.
39. Jalal M, Ramezanianpour AA, Pouladkhan AR, et al. *Application of Genetic Programming (GP) and ANFIS for Strength Enhancement Modeling of CFRP-Retrofitted Concrete Cylinders*, 2013, pp. 455–470. DOI: 10.1007/s00521-012-0941-2.
40. Lim JC, Karakus M and Ozbakkaloglu T. Evaluation of ultimate conditions of FRP-confined concrete columns using genetic programming. *Comput Struct* 2016; 162: 28–37. DOI: 10.1016/j.compstruc.2015.09.005.
41. Mansouri I, Ozbakkaloglu T and Kisi O. Predicting behavior of FRP-confined concrete using neuro fuzzy , neural network , multivariate adaptive regression splines and M5 model tree techniques. *Mater Struct* 2016. DOI: 10.1617/s11527-015-0790-4.
42. Amin R, Biswajit M, Aminul R, et al. Support vector regression approach to predict the strength of frp confined concrete. *Arab J Sci Eng* 2016; 42(3):1129–1146. DOI: 10.1007/s13369-016-2340-y.
43. Cascardi A, Micelli F and Aiello MA. An artificial neural networks model for the prediction of the compressive strength of FRP-confined concrete circular columns. *Eng Struct* 2017; 140: 199–208. DOI: 10.1016/j.engstruct.2017.02.047.
44. Mansouri I, , Kisi O, , Sadeghian P, et al. Applied sciences prediction of ultimate strain and strength of FRP-confined concrete cylinders using. *Appl Sci* 2017; 7(8): 751, doi:10.3390/app7080751.
45. Sharifi Y, Lotfi F and Moghbeli A. Archive of SID compressive strength prediction using the ANN method for FRP confined rectangular concrete columns. *J Rehabil Civil Eng* 2019; 4: 134–153. DOI: 10.22075/JRCE.2018.14362.1260.

46. Naderpour H, Nagai K, Fakharian P, et al. Innovative models for prediction of compressive strength of FRP-confined circular reinforced concrete columns using soft computing methods. *Compos Struct* 2019. DOI: 10.1016/j.compstruct.2019.02.048.
47. Kamgar R, Naderpour H, Komeleh HE, et al. A proposed soft computing model for ultimate strength estimation of FRP-confined concrete cylinders. *Appl Sci* 2020; 10(5): 1769. DOI: 10.3390/app10051769.
48. Hamid FL, Bahroz G and Sardasht J. Predicting ultimate strength of FRP and lateral steel confined circular concrete columns using artificial neural networks. *Asian J Civ Eng* 2020: 0123456789. DOI: 10.1007/s42107-020-00328-x.
49. Ahmad A and Plevris V. Prediction of properties of FRP-confined concrete cylinders based on artificial neural networks. *Crystal* 2020; 10(9): 811.
50. Keshtegar B, Gholampour A, Thai DK, et al. Hybrid regression and machine learning model for predicting ultimate condition of FRP-confined concrete. *Compos Struct* 2021; 262: 113644. DOI: 10.1016/j.compstruct.2021.113644.
51. Al-Salloum YA. Influence of edge sharpness on the strength of square concrete columns confined with FRP composite laminates. *Compos B Eng* 2007; 38(5–6): 640–650. DOI: 10.1016/j.compositesb.2006.06.019.
52. Benzaid R, Chikh NE and Mesbah H. Behaviour of square concrete column confined with GFRP composite WARP. *J Civ Eng Manag* 2008; 14(2): 115–120. DOI: 10.3846/1392-3730.2008.14.6.
53. Campione G. Influence of FRP wrapping techniques on the compressive behavior of concrete prisms. *Cem Concr Compos* 2006; 28(5): 497–505. DOI: 10.1016/j.cemconcomp.2006.01.002.
54. Campione G, Miraglia N and Scibilia N. Compressive behavior of R.C. members strengthened with carbon fiber reinforced plastic layers. *Adv Earthq Eng* 2001; 9: 397–406.
55. Carrazedo R. *Mechanisms of Confinement and its Implication in Strengthening of Concrete Columns with FRP Jacketing*. University of Sao Paulo, 2002.
56. Chaallal O, Shahawy M, and Hassan M, Performance of axially loaded short rectangular columns strengthened with carbon fiber-reinforced polymer wrapping, *J Compos Constr* 2003; 7(3): 200–208. DOI: 10.1061/(ASCE)1090-0268(2003)7:3(200).
57. Demers M and Neale KW. Strengthening of Concrete Columns with Unidirectional Composite Sheets, 1994.
58. Erdil B, Akyuz U and Yaman IO. Mechanical behavior of CFRP confined low strength concretes subjected to simultaneous heating-cooling cycles and sustained loading. *Mater Struct Constr* 2012; 45(1–2): 223–233. DOI: 10.1617/s11527-011-9761-6.
59. Harries KA and Carey SA. "Shape and 'gap' effects on the behavior of variably confined concrete. *Cem Concr Res* 2003; 33(6): 881–890. DOI: 10.1016/S0008-8846(02)01085-2.
60. Hosotani M, Kawashima K and Hoshikuma J. "A model for confinement effect for concrete cylinders confined by carbon fiber sheets," In Workshop on Earthquake Engineering Frontiers of Transportation Facilities, (1997.405–430. Accessed: Apr. 30, 2021. [Online]. Available:, https://trid.trb.org/view/487424
61. Ignatowski P and Kamińska ME. On the effect of confinement of slender reinforced concrete columns with CFRP composites. *Eng Build I Budownictwa)* 2003; 4: 204–208, Accessed: Apr. 30, 2021. [Online]. Available: https://www.researchgate.net/publication/41650200_On_the_effect_of_confinement_of_slender_reinforced_concrete_columns_with_CFRP_composites.
62. Masia MJ, Gale TN and Shrive NG. Size effects in axially loaded square-section concrete prisms strengthened using carbon fibre reinforced polymer wrapping. *Can J Civ Eng* 2004; 31(1): 1–13. DOI: 10.1139/l03-064.
63. Mirmiran A, Shahawy M, Samaan M, et al. Effect of column parameters on FRP-confined concrete. *J Compos Constr* 1998; 2(4): 175–185. DOI: 10.1061/(ASCE)1090-0268.
64. Modarelli R, Micelli F, and Manni O, "FRP-Confinement of Hollow Concrete Cylinders and Prisms," in Proceedings of the 7th International Symposium on Fiber Reinforced Polymer Reinforcement of Reinforced Concrete Structures, 2005, pp. 1029–1046.
65. Parvin A and Wang W. Behavior of FRP jacketed concrete columns under eccentric loading. *J Compos Constr* 2001; 5(3): 146–152. DOI: 10.1061/(ASCE)1090-0268.
66. Rochette P and Labossière P. Axial testing of rectangular column models confined with composites. *J Compos Constr* 2000; 4(3): 129–136. DOI: 10.1061/(ASCE)1090-0268.
67. Rousakis TC, Karabinis AI and Kiousis PD. FRP-confined concrete members: Axial compression experiments and plasticity modelling. *Eng Struct* 2007; 29(7): 1343–1353. DOI: 10.1016/j.engstruct.2006.08.006.
68. Rousakis TC and Karabinis AI. Adequately FRP confined reinforced concrete columns under axial compressive monotonic or cyclic loading. *Mater Struct Constr* 2012; 45(7): 957–975. DOI: 10.1617/s11527-011-9810-1.
69. Shehata IAEM, Carneiro LAV and Shehata LCD. Strength of short concrete columns confined with CFRP sheets. *Mater Struct Constr* 2002; 34(245): 50–58. DOI: 10.1007/bf02482090.
70. Suter R., Pinzelli R. and of Cambridge U. "Confinement of concrete columns with FRP sheets," in Proceedings of the 5th Symposuim on Fibre Reinforced Plastic Reinforcement for Concrete Structures, 2001, pp. 793–802.
71. Tao Z, Yu Q and Zhong Y-Z. Compressive behaviour of CFRP-confined rectangular concrete columns. *Mag Concr Res* 2008; 60(10): 735–745. DOI: 10.1680/macr.2007.00115.
72. Wang LM and Wu YF. Effect of corner radius on the performance of CFRP-confined square concrete columns: Test. *Eng Struct* 2008; 30(2): 493–505. DOI: 10.1016/j.engstruct.2007.04.016.
73. Wang Y and Wu H. Experimental investigation on square high-strength concrete short columns confined with AFRP sheets. *J Compos Constr* 2010; 14(3): 346–351. DOI: 10.1061/(asce)cc.1943-5614.0000090.
74. Wang Y and Wu H. Size effect of concrete short columns confined with aramid FRP jackets. *J Compos Constr* 2011; 15(4): 535–544. DOI: 10.1061/(asce)cc.1943-5614.0000178.
75. Wang Z, Wang D and Smith S. Size Effect of Square Concrete Columns Confined with CFRP Wraps, 2012.

76. Wang Z, Wang D, Smith ST, et al. CFRP-Confined Square RC Columns. I: Experimental Investigation. *J Compos Constr* 2012; 16(2): 150–160. DOI: 10.1061/(asce)cc.1943-5614.0000245.
77. Wu YF and Wei YY. Effect of cross-sectional aspect ratio on the strength of CFRP-confined rectangular concrete columns. *Eng Struct* 2010; 32(1): 32–45. DOI: 10.1016/j.engstruct.2009.08.012.
78. Yan Z, Pantelides CP and Reaveley LD. Fiber-reinforced polymer jacketed and shape-modified compression members: I - Experimental behavior. *ACI Struct J* 2006; 103(6): 885–893.
79. Yeh FY and Chang KC. Size and shape effects on strength and ultimate strain in frp confined rectangular concrete columns. *J Mech* 2012; 28(4): 677–690. DOI: 10.1017/jmech.2012.118.
80. Youssef MN, Feng MQ and Mosallam AS. Stress-strain model for concrete confined by FRP composites. *Compos Part B Eng* 2007; 38(5–6): 614–628. DOI: 10.1016/j.compositesb.2006.07.020.
81. Zhang DJ, Wang YF and Ma YS. Compressive behaviour of FRP-confined square concrete columns after creep. *Eng Struct* 2010; 32(8): 1957–1963. DOI: 10.1016/j.engstruct.2010.02.023.
82. Ozbakkaloglu T and Oehlers DJ. Concrete-Filled Square and Rectangular FRP Tubes under Axial Compression. *J Compos Constr* 2008; 12(4): 469–477. DOI: 10.1061/(ASCE)1090-0268.124
83. Ozbakkaloglu T. Behavior of square and rectangular ultra high-strength concrete-filled FRP tubes under axial compression. *Compos Part B Eng* 2013; 54(1): 97–111. DOI: 10.1016/j.compositesb.2013.05.007.
84. Ozbakkaloglu T., "Compressive behavior of square and rectangular high-strength concrete-filled FRP tubes," in Proceedings of the 12th International Symposium on Structural Engineering, ISSE 2012, Aug. 2012, 17(1): 965–970, doi: 10.1061/(asce)cc.1943-5614.0000321.
85. Louk Fanggi BA and Ozbakkaloglu T. Square FRP-HSC-steel composite columns: Behavior under axial compression. *Eng Struct* 2015; 92: 156–171. DOI: 10.1016/j.engstruct.2015.03.005.
86. Fallah Pour A, Gholampour A, Zheng J, et al. Behavior of FRP-confined high-strength concrete under eccentric compression: Tests on concrete-filled FRP tube columns. *Compos Struct* Jul. 2019; 220: 261–272. DOI: 10.1016/j.compstruct.2019.03.031.
87. Demir U, Sahinkaya Y, Ispir M, et al. Assessment of axial behavior of circular HPFRCC members externally confined with FRP sheets. *Polymers (Basel)* 2018; 10(2): 138. DOI: 10.3390/polym10020138.
88. Ozbakkaloglu T. Ultra-high-strength concrete-filled frp tubes: Compression tests on square and rectangular columns. *In* Key Eng Mater 2014; 575–576: 239–244. DOI: 10.4028/www.scientific.net/KEM.575-576.239.
89. McCulloch WS and Pitts W. A logical calculus of the ideas immanent in nervous activity. *Bull Math Biophys* 1943; 5(4): 115–133. DOI: 10.1007/BF02478259.
90. Rosenblatt F. The perceptron: A probabilistic model for information storage and organization in the brain. *Psychol Rev* 1958; 65(6): 386–408. DOI: 10.1037/h0042519.
91. Minsky M and Papert SA. *Perceptrons: An Introduction to Computational Geometry*. MIT Press, 2017.
92. Werbos PJ. System Modeling and Optimization. Springer-Verlag, 2005, pp. 762–770.Applications of advances in nonlinear sensitivity analysis,
93. Ouaer H, et al. Rigorous connectionist models to predict carbon dioxide solubility in various ionic liquids. *Appl Sci* 2020; 10(1): 304. DOI: 10.3390/app10010304.
94. Amouei Ojaki H, Lashkarbolook M and Movagharnejad K. Correlation and prediction of surface tension of highly non-ideal hydrous binary mixtures using artificial neural network. *Colloids Surf A Physicochem. Eng. Asp* 2020; 590: 124474. DOI: 10.1016/j.colsurfa.2020.124474.
95. Abdi-Khanghah M, Bemani A, Naserzadeh Z, et al. Prediction of solubility of N-alkanes in supercritical CO2 using RBF-ANN and MLP-ANN. *J CO2 Util* 2018; 25: 108–119. DOI: 10.1016/j.jcou.2018.03.008.
96. Ghritlahre HK and Prasad RK. Exergetic performance prediction of solar air heater using MLP, GRNN and RBF models of artificial neural network technique. *J Environ Manage* 2018; 223: 566–575. DOI: 10.1016/j.jenvman.2018.06.033.
97. Afshin T, et al. Prediction of water formation temperature in natural gas dehydrators using radial basis function (RBF) neural networks. *Nat Gas Ind B* 2016; 3(2): 173–180. DOI: 10.1016/j.ngib.2016.06.002.
98. Du KL and Swamy MNS. *Neural Networks in a Softcomputing Framework*. Springer London, 2006.
99. Wu Y, Zhang B and Du KL. Using radial basis function networks for function approximation and classification. *ISRN Appl Math* 2012; 2012: 1–34.
100. Elzwayie A, El-shafie A, Yaseen ZM, et al. "RBFNN-based model for heavy metal prediction for different climatic and pollution conditions," *Neural Comput Appl*, vol. 28, no. 8, pp. 1991–2003, Aug. 2017, doi: 10.1007/s00521-015-2174-7.
101. Yuvaraj P, Ramachandra Murthy A, Iyer NR, et al. Support vector regression based models to predict fracture characteristics of high strength and ultra high strength concrete beams. *Eng Fract Mech* 2013; 98(1): 29–43. DOI: 10.1016/j.engfracmech.2012.11.014.
102. Durgam S, Bhosale A, Bhosale V, et al. Support vector regression method for predicting temperatures of heat sources cooled by forced convection in a horizontal channel. *Therm Sci Eng Prog* 2020; 20: 100725. DOI: 10.1016/j.tsep.2020.100725.
103. Owolabi TO, Akande KO and Olatunji SO. Computational intelligence approach for estimating superconducting transition temperature of disordered MgB 2 superconductors using room temperature resistivity. *Appl Comput Intell Soft Comput* 2016; 2016: 1–7. DOI: 10.1155/2016/1709827.
104. Owolabi T. O. Modeling the magnetocaloric effect of manganite using hybrid genetic and support vector regression algorithms. *Phys Lett Sect A Gen At. Solid State Phys* 2019; 383(15): 1782–1790. DOI: 10.1016/j.physleta.2019.02.036.
105. Vapnik V. N. An overview of statistical learning theory. *IEEE Trans Neural Networks* 1999; 10(5): 988–999. DOI: 10.1109/72.788640.

106. Mokhtari S and Mooney MA. Predicting EPBM advance rate performance using support vector regression modeling. *Tunn Undergr Sp Technol* 2020; 104: 103520. DOI: 10.1016/j.tust.2020.103520.
107. Sun J, Zhang J, Gu Y, et al. Prediction of permeability and unconfined compressive strength of pervious concrete using evolved support vector regression. *Constr Build Mater* 2019; 207: 440–449. DOI: 10.1016/j.conbuildmat.2019.02.117.
108. El Amine Ben Seghier M, Keshtegar B, Tee KF, et al. Prediction of maximum pitting corrosion depth in oil and gas pipelines. *Eng Fail Anal* 2020; 112: 104505. DOI: 10.1016/j.engfailanal.2020.104505.
109. Ben Seghier MEA, Corriea JAFO, Jafari-Asl J, et al. On the modeling of the annual corrosion rate in main cables of suspension bridges using combined soft computing model and a novel nature-inspired algorithm. *Neural Comput Appl* 2021; 0123456789. DOI: 10.1007/s00521-021-06199-w.